Published in final edited form as:
J Immunol. 2006 April 15; 176(8): 4826–4833.

In Vivo Recognition of Ovalbumin Expressed by Transgenic *Leishmania* Is Determined by Its Subcellular Localization1

Sara Prickett[2,*,†], **Peter M. Gray**[‡], **Sara L. Colpitts**[‡], **Phillip Scott**[‡], **Paul M. Kaye**[2,†], and **Deborah F. Smith**[2,3,*]

[*]Wellcome Trust Laboratories for Molecular Parasitology, Centre for Molecular Microbiology and Infection, Imperial College, London, United Kingdom;

[†]Department of Infectious and Tropical Diseases, London School of Hygiene and Tropical Medicine, London, United Kingdom;

[‡]Department of Pathobiology, School of Veterinary Medicine, University of Pennsylvania, Philadelphia, PA 19104

Abstract

The importance of the site of Ag localization within microbial pathogens for the effective generation of $CD8^+$ T cells has been studied extensively, generally supporting the view that Ag secretion within infected target cells is required for optimal MHC class I-restricted Ag presentation. In contrast, relatively little is known about the importance of pathogen Ag localization for the activation of MHC class II-restricted $CD4^+$ T cells, despite their clear importance for host protection. We have used the N-terminal targeting sequence of *Leishmania major* hydrophilic acylated surface protein B to generate stable transgenic lines expressing physiologically relevant levels of full-length OVA on the surface of metacyclic promastigotes and amastigotes. In addition, we have mutated the hydrophilic acylated surface protein B N-terminal acylation sequence to generate control transgenic lines in which OVA expression is restricted to the parasite cytosol. In vitro, splenic dendritic cells are able to present membrane-localized, but not cytosolic, OVA to OVA-specific DO.11 T cells. Strikingly and unexpectedly, surface localization of OVA is also a strict requirement for recognition by OVA-specific T cells (DO.11 and OT-II) and for the development of OVA-specific Ab responses in vivo. However, recognition of cytosolic OVA could be observed with increasing doses of infection. These data suggest that, even under in vivo conditions, where varied pathways of Ag processing are likely to operate, the site of *Leishmania* Ag localization is an important determinant of immunogenicity and hence an important factor when considering the likely candidacy of vaccine Ags for inducing $CD4^+$ T cell-dependent immunity.

[3] Address correspondence and reprint requests to Dr. Deborah F. Smith, Immunology and Infection Unit, Department of Biology/Hull York Medical School, University of York, Heslington, York YO10 5YW, U.K. E-mail address: dfs501@york.ac.uk.

[1]This work was supported by Wellcome Trust Grant 061343 (to D.F.S.), UK Medical Research Council Grant G981148 (to P.M.K.), and National Institutes of Health Grant AI35914 (to P.S.). S.P. was the recipient of a Postgraduate Student Bursary from the Biochemistry Department, Imperial College London; and P.M.G. was the recipient of a National Institutes of Health National Training Award (Grant AI07518).

[2]Current addresses: S.P., Division of Infection and Immunity, Walter and Eliza Hall Institute, Royal Parade, Parkville VIC 3050, Australia; P.M.K. and D.F.S., Immunology and Infection Unit, Department of Biology/Hull York Medical School, University of York, Heslington, York YO10 5YW, U.K.

Disclosures
The authors have no financial conflict of interest.

Europe PMC Funders Author Manuscripts

Ag processing is an important first step in the initiation of $CD4^+$ and $CD8^+$ T cell-mediated immunity. Although the biochemical and cell biological principles of Ag processing have been elucidated in a number of model systems (1-4), many of the fundamental issues underlying the recognition of complex pathogens remain to be defined. For example, selection of rational vaccine candidate Ags, to ensure not only immunogenicity but also effective target cell recognition, is dependent on understanding the parameters that affect Ag recognition in vivo. In the context of MHC class I (MHC-I)[4]-restricted Ag recognition, this topic has been studied intensely over the past few years, and data from a number of model systems, both in vitro and in vivo, now indicate the desirability of selecting Ags secreted by intracellular pathogens (5-7). Recent data suggest that initial uptake of pathogens by neutrophils may serve to extend the breadth of Ag recognition and enhance $CD8^+$ T cell responses to nonsecreted proteins (8).

In contrast to these studies on MHC-I-restricted recognition, it remains unclear how the subcellular localization of Ag in pathogens affects subsequent induction of MHC class II (MHC-II)-restricted $CD4^+$ T cell responses. Early in vitro studies on the recognition of intracellular pathogens, including *Leishmania*, mycobacteria and *Salmonella* (3, 7, 9-12), indicated that Ag localization might be an important factor governing recognition. Thus, recognition of the abundant cysteine proteases of *Leishmania mexicana* (which are located within the parasite's lysosomal compartment) requires parasite killing within macrophage phagosomes to facilitate recognition by a cysteine protease-specific T cell clone (11). In contrast, whereas membrane-bound acid phosphatase (a constituent of intracellular vesicles of the amastigote stage of this parasite) is not recognized by T cells, recognition can be achieved by overexpression at the parasite plasma membrane or, more efficiently, by engineering parasites to express a soluble version of this protein (10, 11). These results have been interpreted as reflecting antigenic competition for a limited availability of MHC-II molecules in APCs, with low abundance or poorly processed Ags being out competed by more abundant or more readily processed Ags (11-13). Although providing valuable information on epitope competition during intracellular Ag processing, these in vitro studies considerably underestimate the complexity of in vivo Ag recognition. For example, it is now well established that dendritic cells (DCs) play an essential role in $CD4^+$ T cell priming (14), and the IFN-γ-stimulated bone marrow-derived macrophages used in these earlier studies would be expected to express relatively low levels of MHC-II and display differing Ag processing characteristics to DCs. These conditions, coupled with supraphysiological levels of Ag expression, may have favored antigenic competition. Furthermore, it is now known that Ag acquisition by DCs in vivo also may be indirect, reflecting uptake and degradation of apoptotic infected cells (15). Unfortunately, the half-life of most physiologically relevant DC subsets is short ex vivo (16), infection levels are variable depending on the subset studied (17, 18) and appropriate levels of Ag exposure such as would be achieved in vivo are difficult to reproduce in vitro, necessitating alternative approaches to address the importance of subcellular distribution of parasite Ag in generating in vivo immune responses.

To further clarify the importance of subcellular Ag distribution for the in vivo immunogenicity of *Leishmania* proteins, we have therefore adopted a molecular approach to generate fully infective transgenic (Tg) *L. major* expressing OVA at physiological levels in different subcellular compartments. Our data indicate that, during the initiation of a *L. major* infection in the footpad, OVA expressed on the *L. major* plasma membrane, but not as a cytosolic protein, can be recognized by naive $CD4^+$ T cells in vivo. Recognition of cytosolic

[4]Abbreviations used in this paper: MHC-I, MHC class I; MHC-II, MHC class II; CPBIR, cysteine proteinase B intergenic region; HASPB, hydrophilic acylated surface protein B; NMT, *N*-myristoyl transferase; DC, dendritic cell; Tg, transgenic; ORF, open reading frame; PFA, paraformaldehyde; WT, wild type.

OVA occurs only at increasingly high infectious dose. Our data suggest that, even in vivo, a sparse population of *Leishmania* surface proteins may acquire relative immunodominance due to increased Ag accessibility for Ag processing.

Materials and Methods

Mice

BALB/c mice were purchased from Charles River Laboratories or The Jackson Laboratory. DO11.10 TCR Tg mice (19) on a wild-type (WT), SCID, or RAG1$^{-/-}$ background were obtained from F. Powrie (Oxford University, Oxford, U.K.) and C. Hunter (University of Pennsylvania, Philadelphia, PA), through the National Institute of Allergy and Infectious Disease exchange program. OTII TCR Tg mice were obtained from E. Pearce (University of Pennsylvania, Philadelphia, PA). Mice were maintained under barrier conditions with free access to food and water. Animal experiments were conducted following the guidelines of the London School of Hygiene and Tropical Medicine and the University of Pennsylvania institutional animal care and use committees (and under UK Home Office license). Experimental groups were age- and sex-matched, being 6–10 wk old at the onset of the experiments.

Parasites and infections

L. major Friedlin clone V1 (FV1) (MHOM/IL/80/Friedlin) promastigotes were cultured at 26°C in Schneider's *Drosophila* medium (Invitrogen Life Technologies) supplemented with 15% (v/v) FCS and 100 U/ml penicillin/streptomycin. Infective metacyclic promastigotes were purified from stationary-phase cultures by negative selection with peanut lectin (Sigma-Aldrich) as described (20). For passage and to test infectivity of clones, groups of BALB/c mice were infected s.c. in one hind footpad with 10^6 metacyclics. Lesion size was measured at regular intervals (using Vernier calipers) and normalized to the uninfected hind footpad. Limiting dilution assays were performed as described previously (21, 22). To harvest amastigotes, lesions were processed (21), and larger debris was removed (by centrifugation at 100 × *g* for 10 min) before parasite/host cell retrieval (at 2200 × *g*) and cell lysis in 0.05% saponin. Released amastigotes were washed and used immediately.

Construct assembly

The first 18 codons of *L. major* hydrophilic acylated surface protein B (HASPB) plus ~50 bp of upstream sequence were PCR amplified from the *HASPB* gene (accession no. AJ237587) using primers CCGTGCGCTCGAGTGATCCTATCTATCTCC and TAGAGGATCCATCCGCACTTTTCTGGGGCTC, before cloning via *Xho*I/*Bam*HI sites into the multiple cloning site of pSSU-int (23). In all primers, restriction sites used for cloning are underlined. A second construct was made to substitute Ala for Gly at position 2 of the HASPB N terminus (HASP/GA), using the alternate forward primer, ATACTCGAGGCTTATACACCATGGCAAGCTCTTGC. The 1.3-Kb cysteine proteinase B intergenic region (CPBIR) was amplified from pSSU-int with primers TAATGGATCCACCGGTGCCCTTGTGTGCGTGTGT and TAATACTAGTATCGATCGCGGACGCGGGCAG and cloned downstream of the HASPB sequences with *Bam*HI/*Spe*I. Finally, the 1.2-Kb OVA open reading frame (ORF) (accession no. V00383; Ref 9) was amplified, omitting the start codon, using primers GCTAAGGATCCGGCTCCATCGGCGCAGCAA and CAATGCACCGGTAGTTAAGGGGAAACACATCTGCC. This fragment was cloned between the HASPB and CPBIR sequences using *Bam*HI/*Age*I, generating a HASPB-OVA gene fusion, linked in frame by two codons within the *Bam*HI site. Following sequencing, constructs were linearized with *Pac*I/*Pme*I and transfected into *L. major* to generate the Tg lines, PHOC (p-HASP-OVA-CPBIR) and PHOC/GA (p-HASP/GA-OVA-CPBIR) using

standard procedures (23, 24). Successful integration was assessed by PCR and DNA blotting using the 360-bp *Sac*I fragment of the OVA ORF to probe genomic DNA digested with *AgeI.*

Determination of OVA expression

Log-phase promastigotes or purified metacyclics were washed in PBS, re-suspended at 2 × 10^8/ml in PBS/1% Nonidet P40/complete mini protease inhibitor mixture for lysis, and stored at −80°C as described previously (24, 25). Lesion-derived amastigotes were prepared in the presence of 0.4% Triton X-100, 100 μg/ml leupeptin, 500 μg/ml pefabloc, 5 μg/ml pepstatin A, 1 mM 1,10-phenanthroline, 1 mM EDTA/1 mM EGTA, and 25 μg/ml E64 to prevent excessive degradation by high levels of amastigote proteolytic enzymes (26). After four rounds of rapid freeze-thawing and three 10-s bursts of sonication, amastigote lysates were used immediately for immunoblotting or stored at −80°C. Membrane and cytosolic protein fractions were prepared as described before immunoblotting (27). Primary Abs used were polyclonal goat anti-OVA (1/400; Sigma-Aldrich), polyclonal rabbit anti-OVA (1/400; Sigma-Aldrich), polyclonal rabbit anti-*N*-myristoyl transferase (NMT) (1/2000; Ref. 28), or mouse anti-GP63 mAb (1/10; a gift from R. McMaster, University of British Columbia, Vancouver, British Columbia, Canada). Secondary Abs used were anti-rabbit IgG-HRP (1/16,000; Sigma-Aldrich), anti-goat IgG-HRP (1/80,000; Sigma-Aldrich), or anti-mouse IgG-HRP (1/10,000; Jackson ImmunoResearch Laboratories). Detection was performed using ECL (Amersham Biosciences), and membranes were stripped for reprobing using Restore stripping buffer (Pierce) according to the manufacturer's instructions. Surface-exposed proteins were detected by biotinylation as described previously (27). Total Ab-detectable OVA was determined using a capture ELISA in two independent experiments (9).

Fluorescent microscopy

Parasites were fixed in 3% paraformaldehyde (PFA) for 30 min on ice, pipetted on to polylysine-coated slides, and blocked (PBS/5% FCS/0.1% Triton X-100) before labeling with polyclonal goat anti-OVA (1/100; Sigma-Aldrich). Secondary detection used either FITC-conjugated anti-goat IgG (1/100; BD Pharmingen) or biotinylated rabbit anti-goat $F(ab')_2$ (1/100; Molecular Probes), followed by Alexa 488-conjugated streptavidin (1/100; Serotec). Slides were mounted, viewed, and images captured as described previously (27).

Flow cytometry

Log-stage promastigotes or purified metacyclics were fixed in PFA as above, washed in FACS buffer (PBS/1% horse serum (Sigma-Aldrich)/0.1% sodium azide), and blocked in FACS buffer containing 20% horse serum. Parasites were washed either in normal FACS buffer or in FACS buffer containing 0.1% saponin before incubation with goat anti-OVA (1/100; Sigma-Aldrich), followed by FITC-conjugated anti-goat IgG (1/100; BD Biosciences). Samples were analyzed using a FACScan with Cell Quest software (BD Biosciences).

Determination of anti-OVA IgG responses

Serum IgG1 and IgG2a Ab responses were determined by ELISA as described elsewhere (29).

OVA-specific T cell responses

Splenic DCs were used as APCs. BALB/c spleens were digested with 100 μg/ml collegenase D and 100 μg/ml DNase (Worthington/Lorne Laboratories) in RPMI 1640 medium for 10 min at 37°C. Digestion was terminated using RPMI 1640 medium supplemented with 10% FCS (Invitrogen Life Technologies), 100 μg/ml penicillin, 100U/ml

streptomycin, and 10 mM EDTA, and the tissue was passed through a 100-μM Nitex mesh (BD Biosciences). Cells were collected at 1200 rpm, washed twice in MACS buffer (PBS and 1% BSA), and DCs were positively selected using anti-CD11c MACS beads and MS columns (Miltenyi Biotec) per the manufacturer's instructions. DCs were irradiated (2000 rad) before use. $H2A^d$-$OVA_{323–339}$-specific T cells were isolated from DO.11 SCID TCR Tg mice (as described in the *Results*) using anti-CD4 MACS beads. A total of 5×10^4 DCs were mixed with different promastigote preparations (PFA-fixed, freeze-thawed, or whole cell lysate) or 100 μg/ml chicken OVA in U-bottom, 96-well plates (Helena Biosciences) before the addition of 1×10^5 T cells. After 76 h at 37°C/5% CO_2, 1 μCi/well [^{3}H]thymidine was added for 20 h. Plates were harvested onto printed filter mats (PerkinElmer) using a Tomtec cell harvester, and radioactive incorporation was determined using a Microbeta plate reader (Wallac/PerkinElmer). For in vivo studies, whole splenocytes from naive DO.11 (Thy1.2) mice were labeled with CFSE (30) and adoptively transferred (5×10^6 per mouse) into naive BALB. Thy1.1 congenic recipients. Twenty-four hours later, mice were infected s.c. in the footpad with 10^6–2.5×10^7 Tg *L. major*. After 72–96 h, popliteal lymph nodes were removed, and CFSE expression on gated $CD4^+Thy1.2^+$ cells was analyzed by flow cytometry using appropriately conjugated anti-CD4 and anti-Thy1.2 mAbs (RM4-5 and 53-2.1, respectively; BD Pharmingen). Intracellular IFN-γ was determined as described (31).

Statistical analysis

Where applicable, data are expressed as the mean ± SD or SEM. To test significance, Student's unpaired *t* tests were performed. A value of $p \leq 0.05$ was considered significant.

Results

Generation of OVA-expressing *L. major*

Tg parasites expressing HASPB-OVA fusion proteins were generated by homologous recombination using the vector pSSU-int to target transgenes into the ribosomal RNA locus (23). Targeted integration immediately downstream of a RNA polymerase (pol) I promoter (the strongest transcriptional promoter so far identified in *Leishmania*) overcomes the problems of variable protein expression levels and plasmid copy number associated with the use of episomal plasmids (6, 9, 23, 32). Next, 3′UTR sequences from the *L. mexicana* cysteine proteinase B 2.8 gene cluster (CPB IR) were inserted downstream of all gene constructs to support protein expression during amastigote stages of the *Leishmania* life cycle (33).

Two main *HASPB-OVA* gene fusions were designed and assembled for expression in *L. major* (Fig. 1). The first linked the sequence encoding the *L. major* HASPB N-terminal 18 amino acids to the *OVA* ORF to generate the Tg line *Lmj^18SrRNA::HASPB18OVA* (hereafter referred to as PHOC *L. major*), with the prediction that OVA expressed in these parasites would be exported via the HASPB pathway and expressed among the repertoire of surface proteins. The second fusion differed only by a single base substitution in the second codon of the *HASPB* sequence (*GGA* to *GCA*) to encode a Gly-to-Ala switch, generating the Tg line *Lmj^18SrRNA::haspb18OVA* (hereafter referred to as PHOC/GA). This mutation inactivates the *N*-myristoylation site in the targeting sequence, resulting in protein mis-localization to the cytosol (27). Genomic integration of both transgenes was confirmed by PCR amplification (as described previously; Ref. 23) and Southern blotting of *Age I*-digested genomic DNA with the *OVA* ORF (data not shown).

OVA expression in PHOC and PHOC/GA *L. major*

Independent clones of both Tg lines were tested for OVA expression by immunoblotting whole parasite lysates with anti-OVA Abs, using WT *L. major* FV1 lysate and purified OVA as negative and positive controls, respectively. OVA was detected in log-stage promastigotes (Fig. 2*A*) and in lesion-derived amastigotes (Fig. 2*B*) of each Tg line, demonstrating constitutive expression through the parasite life cycle. OVA expression levels showed little variation following repeated in vivo passages through BALB/c mice in the absence of drug selection, as expected given the chromosomal integration site of the transgenes. Compared with the constitutively expressed protein, NMT, densitometric measurements from the immunoblots showed that equivalent levels of OVA were detected in all life-cycle stages. Expression levels in metacyclic promastigotes, determined in multiple experiments, ranged from 1 to 5×10^5 molecules per cell (equivalent to ~3–40 ng of OVA per 10^6 parasites) with no significant differences detected between the levels of OVA expression in PHOC and PHOC/GA *L. major* ($2.9 \pm 2.4 \times 10^5$ vs $2.4 \pm 1.7 \times 10^5$ molecules of OVA per cell, respectively). These values for OVA expression may underestimate the total pool of OVA available for T cell recognition, if partial proteolysis of endogenous OVA had occurred, rendering this material unavailable for recognition by OVA-specific Abs. HASPB levels also were determined (by ELISA) in lysates of PHOC, PHOC/GA, and WT *L. major* to confirm that expression of the HASPB-OVA fusion proteins did not alter significantly the abundance of this endogenous protein (data not shown).

Subcellular localization of OVA in PHOC and PHOC/GA *L. major*

To determine the cellular localization of OVA in these Tg lines, FACS analysis was performed (Fig. 3, *upper panel*). Analysis of fixed log-stage promastigotes indicated that PHOC *L. major*, but not WT or PHOC/GA *L. major*, expressed OVA at the cell surface. To determine whether OVA was localized intracellularly in PHOC/GA *L. major,* promastigotes were permeabilized with saponin before staining. This treatment revealed significant expression of OVA in PHOC/GA *L. major*, compared with WT parasites. However, the equivalent levels of OVA expression observed in permeabilized and nonpermeabilized PHOC *L. major* promastigotes suggested that most of the OVA in this line was expressed at the cell surface. Equivalent data were obtained using metacyclic promastigotes. Analysis of amastigotes by FACS was difficult to interpret because of residual tissue debris (data not shown).

To further define the localization of OVA in these parasites and to examine expression in amastigotes, we used fluorescence microscopy (Fig. 3, *lower panel*). Whereas expression was localized to the plasma membrane, flagella pocket, and flagellum (as well as the cytosol) in PHOC *L. major*, OVA staining was confined to the cytosol in PHOC/GA *L. major*, appearing punctate in appearance, particularly in amastigotes.

The intracellular distribution of OVA was also confirmed by subcellular fractionation followed by immunoblotting. As shown in Fig. 4*A*, 60–70% of detectable OVA was estimated to be membrane associated in PHOC *L. major*, whereas all OVA was localized to the cytosolic fraction in PHOC/GA *L major*. Probing for the GPI-anchored surface glycoprotein, GP63, demonstrated equivalent loading of the different samples, provided a positive marker for the membrane fractions, and confirmed the absence of membrane proteins in the cytosolic fractions. Finally, we used biotinylation to detect proteins exposed on the surface of live parasites (Fig. 4*B*). Promastigotes were incubated with membrane-impermeable NHS-SS-biotin, and then extracellular biotinylated proteins were separated from nonbiotinylated intracellular proteins. By this analysis, up to 45% of OVA detected in PHOC *L. major* was accessible to biotinylation at the external surface of the plasma

membrane. In contrast, no biotinylated OVA was detected in PHOC/GA *L. major*. Control blotting of cytosolic NMT confirmed comparable sample loading and the selectivity of the labeling procedure. Collectively, these data demonstrate the differential targeting of OVA to the external surface or the cytosol, achieved by using native or mutant HASPB targeting sequences.

Growth, differentiation, and infectivity of PHOC and PHOC/GA *L. major*

Before investigation of the immune responses induced by infection with the PHOC *L. major* and PHOC/GA *L. major*, it was essential to demonstrate that genetic manipulation had not affected the ability of these cells to grow, differentiate, and acquire infectivity in vivo. To this end, clones of both Tg lines were cultured in vitro, following their first passage through BALB/c mice, and showed equivalent growth rates and differentiation profiles when compared with WT *L. major* (data not shown). Both Tg lines were also tested for virulence using differentiated metacyclic promastigotes to infect BALB/c mice (Fig. 5). No significant differences were detected between the size or parasite loads of lesions following inoculation with PHOC, PHOC/GA, or WT *L. major.* Thus, these cloned parasites could be used comparatively to directly assess the role of Ag localization on immune responses following in vivo infection.

Recognition of Tg *L. major* by DO11 T cells

Because DCs are critical for the priming of naive $CD4^+$ T cells, and MHC-II expression on DCs is sufficient to direct the T cell response to *L. major* in vivo (14), we first determined whether the HASPB-OVA fusion proteins expressed by PHOC and PHOC/GA *L. major* could be processed by DCs into the appropriate peptides for recognition by DO11.10 $CD4^+$ T cells. Fresh splenic DCs pulsed with PHOC *L. major* induced significant dose-dependent proliferation of DO11.10 T cells (Fig. 6*A*), clearly demonstrating that $OVA_{323–339}$ epitopes can be processed and presented from these parasites. As expected, no response was elicited by DCs pulsed with WT *L. major*. However, more significantly, we were unable to elicit responses using DCs pulsed with fixed PHOC/GA *L. major* promastigotes, suggesting that the intracellular location of OVA in these parasites was not compatible with optimal Ag processing. Similar data were obtained using heat-treated promastigotes (data not shown). We next compared the response elicited by freeze-thawed parasites and soluble parasite lysate to determine whether these methods of Ag preparation would enhance recognition of OVA in PHOC/GA *L. major*. Collectively, the results of these experiments (Fig. 6) indicated that 1) recognition of OVA from PHOC *L. major* was optimal when fixed promastigotes were used, and that 2) differential recognition of OVA in PHOC/GA *L. major* was retained even using freeze-thawed parasites or soluble lysates. Given that the HASPB-OVA fusion protein in PHOC/GA *L. major* differed from that in PHOC *L. major* by only one residue in the HASPB N terminus, absence of proliferation could not be attributed to a lack of OVA epitopes. Instead, these data suggest that accessibility of the expressed OVA for processing and/or Ag competition may play a large part in determining the immunogenicity of OVA expressed by these two Tg lines.

HASPB-mediated localization of OVA in PHOC *L. major* determines recognition in vivo

Following footpad infection with 10^6 metacyclic promastigotes, proliferation of DO.11 T cells was observable only in mice infected with PHOC *L. major* and not with PHOC/GA *L. major* or WT parasites (Fig. 7), mirroring the data obtained in our in vitro studies (Fig. 6). To ascertain whether increasing the infective dose would expose a response to cytosolic OVA, mice also were infected with increasing doses of promastigotes (up to 2.5×10^7). As shown in Fig. 7, recognition of cytosolic OVA could be observed following higher-dose infection, albeit at a consistently lower level than that for OVA expressed on the plasma membrane of PHOC *L. major*. Similar results were obtained with OTII cells on a C57BL/6

background, demonstrating that recognition of OVA occurs in both susceptible (BALB/c) and resistant (C57BL/6) mice (Fig. 8). To determine whether recognition of OVA Tg parasites was also associated with cytokine production, we measured intra-cellular IFN-γ in OT-II cells following infection of mice with PHOC and PHOC/GA *L. major*. As expected from previous studies (34), IFN-γ production was linked to cell division, with the capacity of OT-II cells to produce IFN-γ, in response to either OVA-IFA or to infection with PHOC *L. major*, increasing substantially after three cell divisions (Fig. 8). IFN-γ production following infection with PHOC/GA *L. major* was substantially reduced, compared with infection with PHOC *L. major*, in keeping with the lower frequency of cells that had progressed through multiple cell divisions (Fig. 8, *top right panel*). Thus, as measured by both proliferation and IFN-γ production in vivo, the site of OVA expression in *Leishmania* parasites plays a major role in governing the immunogenicity of this molecule.

Finally, we wished to examine the responses to these parasites under conditions where OVA-specific T cells were not exaggerated by adoptive transfer of TCR Tg T cells. Hence, we infected normal BALB/c mice and measured T cell-dependent, isotype-specific anti-OVA responses (35) in mice infected with these Tg lines. No OVA-specific IgG1 or IgG2a was detected following infection with 10^6 WT parasites, as expected. In contrast, following infection with PHOC *L. major*, levels of OVA-specific IgG1 were significant by week 2 postinfection and increased with time thereafter. OVA-specific IgG2a Abs were significantly elevated only at week 6 post infection, but again increased thereafter (Fig. 9). Strikingly, even though parasites persisted and increased in number over the infection period from 10^6 to > 10^{10} per mouse at day 45 (Fig. 5), mice infected with PHOC/GA *L. major* failed to mount any significant IgG1 or IgG2a response at any of the time points examined (Fig. 9 and data not shown). These data indicate that expression of OVA at the parasite surface is a requirement for effective activation of $CD4^+$ T cell-dependent responses in normal mice, even under conditions of extensive parasite multiplication within the host and with a diverse repertoire of potential APC and Ag processing pathways.

Discussion

The importance of Ag localization for in vivo MHC-I-restricted Ag recognition of *Leishmania* proteins has not been examined previously. In this study, we have generated novel Tg lines of *L. major*, using an unusual *Leishmania* plasma membrane targeting sequence, and demonstrated that surface localization of OVA is essential for immunogenicity in vivo. These data extend previous in vitro observations that suggested an important role for subcellular distribution of Ag in parasites as a determinant of antigenic competition for MHC-II molecules in macrophages (10, 11, 13) and indicate that similar phenomena may operate even in the context of a complex and dynamic APC response to infection.

The generation of Tg *Leishmania* expressing various immunological “reporter” proteins has been reported previously and such parasites used to evaluate various parameters of MHC-I- and MHC-II-restricted Ag presentation (9). Indeed, a recent study has confirmed that secretion of OVA by Tg *L. major* is essential for optimal in vitro and in vivo recognition by $CD8^+$ T cells (36). However, in this and most other cases, episomal expression systems have been used, leading to potential loss of transgene-encoding episomes during drug-free multiplication of parasites in the mammalian host. This has restricted use of these parasites for long-term evaluation of immune responses in vivo. As an alternative strategy, we have therefore generated a transgene to encode OVA fused to the N-terminal 18aa of the endogenous HASPB protein of *L. major* and targeted this sequence to the rDNA chromosomal locus using the genomic integrating vector, pSSU-int (23), to achieve consistent levels of expression in all stages of the parasite life cycle. The HASP proteins,

found only in *Leishmania* species, are dual acylated infective-stage molecules that contain an *N*-myristoylation site within the N-terminal 18aa, an essential requirement for the cotranslation acylation of HASPB and subsequent targeting to the plasma membrane and external surface of *Leishmania* (27). Expression of GFP fused to this N-terminal domain facilitates targeting of fluorescent protein to the plasma membrane of mammalian cells via a novel endoplasmic reticulum-independent pathway (27, 37). Studies of HASPB-GFP fusion proteins in both *L. major* and in mammalian cells have confirmed the importance of this targeting domain and shown that introduction of a Gly-to-Ala substitution at position 2 of the HASPB N terminus prevents *N*-myristolation at this site, causing HASPB-GFP to mislocalize to the cytoplasm.

The successful generation of Tg lines of *L. major* expressing OVA fused to both the native and mutant N-terminal HASPB domains (PHOC and PHOC/GA *L. major*, respectively) was confirmed by immunochemical and biochemical analysis and directly by microscopy. Equivalent amounts of HASPB-OVA fusion proteins were expressed during all life-cycle stages, and these lines were indistinguishable from WT parasites by all criteria tested, with the exception of OVA localization. As predicted, PHOC *L. major* expressed OVA at the plasma membrane. Surface biotinylation detected a higher percentage of HASP-localized OVA (~45% of total) in PHOC *L. major* than was detected previously for native HASPB in WT parasites (20–30% of total; Ref. 27). This discrepancy could be a consequence of greater exposure of the larger OVA molecule to biotinylation at the surface or may indeed represent differences in the proportion of OVA, compared with endogenous HASPB, that reaches the surface by this route. Further knowledge of the biochemical mechanism(s) by which the HASPB N terminus mediates localization of proteins to the extracellular face of the membrane will be required to determine whether OVA translocates more efficiently than native HASPB. OVA is also detected in smaller amounts in the flagellar pocket and cytosol of PHOC *L. major* (Figs. 3-5), accounting for <30% of the total OVA at any one time. This expression pattern is probably attributable to newly synthesized proteins trafficking to the plasma membrane. Although no OVA was detected in the culture medium of PHOC *L. major* promastigotes, immunoelectron microscopy has suggested that HASPB may be released from amastigotes into the parasitophorous vacuole of infected cells (data not shown). In contrast, OVA fused to the mutant HASPB N terminus remained internally localized in PHOC/GA *L. major* and appeared to be distributed throughout the cytosol, as demonstrated for non-*N*-myristoylated HASPB (27). OVA was expressed in PHOC and PHOC/GA *L. major* at levels similar to that observed for native HASPB (38, 39). Furthermore, expression of the endogenous HASPB in these Tg parasites was unaltered, compared with WT *L. major*, indicating that expression of the HASPB-OVA fusion proteins was not deleterious to the expression of endogenous HASPB (data not shown). Collectively, these data indicate that study of these Tg lines should provide useful clues about not only the basic aspects of Ag recognition but also the immunogenicity of HASPB, a novel vaccine candidate Ag for leishmaniasis (29, 40).

We first determined whether these parasites would stimulate activation of OVA-specific DO.11 T cells in vitro. Using fixed promastigotes to pulse splenic DCs in vitro, the results from these experiments indicated a clear requirement for localization of OVA to the parasite plasma membrane. Indeed, OVA expressed in the parasite cytosol at an equivalent level was not recognized by DO.11 T cells under these conditions. Importantly, although DCs pulsed with lysates of PHOC *L. major* stimulated a weaker response, compared with fixed parasites, use of lysates failed to uncover any response to OVA expressed in PHOC/GA *L. major*. These results suggest that surface localization of OVA in fixed cells might provide a selective advantage in terms of rapid accessibility to the endosomal proteases responsible for Ag processing. Our observation that this selective advantage is maintained even after preparation of freeze-thawed Ag or cell lysates from PHOC parasites might be attributed to

continued membrane association of OVA, facilitating more efficient presentation. Our data do not address whether this might occur at the level of protease activity or at the level of availability of MHC-II molecules for peptide binding. Given that OVA expressed in PHOC *L. major* and PHOC/GA *L. major* differs only in the HASPB N-terminal sequence, we would not anticipate any inherent differences in the processing of OVA per se in these two parasite lines. In a previous study, we demonstrated that expression of OVA in the cytosol of *L. major* LV39 (c5 pX-OV-2) could, however, lead to the activation of primed OVA-specific $CD4^+$ T cells (9). Although OVA expression levels in the PHOC/GA *L. major* parasites used in the current study were ~20-fold higher than those measured in LV39 c5 pX-OV-2, this discrepancy may reflect the differences in threshold number of MHC-II-peptide complexes required for the activation of primed polyclonal T cells, compared with activation of DO.11 T cells obtained from naive DO.11 SCID mice used here. Other as yet uncharacterized differences between the *L. major* strains used (LV39 vs FV1) cannot be formally ruled out.

To assess the in vivo $CD4^+$ T cell response to OVA expressed in *L. major*, we used the adoptive transfer model originally developed by Jenkins and colleagues (41). After footpad infection of mice with 10^6 parasites, adoptively transferred CFSE-labeled, OVA-specific TCR Tg $CD4^+$ T cells were observed to proliferate only following infection with PHOC *L. major*, correlating with our in vitro observations and indicating that cytosolic OVA was poorly recognized, if at all, under these infection conditions. Nevertheless, by increasing the infective dose of Tg parasites, we were able to uncover a response to PHOC/GA *L. major*, although this was always substantially lower than that seen with PHOC *L. major*. Examination of CFSE reduction profiles also indicated that, for any given infection dose, a greater fraction of activated $CD4^+$ T cells underwent multiple cell divisions in mice infected with PHOC *L. major*, compared with PHOC/GA *L. major*. The ability of $CD4^+$ T cells to synthesize IFN-γ is associated with cell division (34), and, consequently, the heightened proliferative response to PHOC *L. major* infection was associated with increased IFN-γ production, compared with infection with PHOC/GA *L. major*. At present, it remains unclear whether the dose effects reported here reflect increased Ag loading within individual APCs in vivo or an increase in the number or type of APCs that participate in the response. In contrast with these studies, the relative ease with which the similarly abundant intracellular *Leishmania* homolog of receptors for activated C kinase Ag of *L. major* is recognized by TCR Tg T cells may reflect specific mechanisms for Ag capture or an unusually high avidity of MHC binding (42, 43).

Our data using TCR Tg T cells indicate that recognition of OVA is clearly influenced by its localization within the parasite, with plasma membrane expression conferring a selective advantage, particularly at the lowest infection doses tested. In this context, the results of infection of normal mice, in which the frequency of OVA-specific T cells is extremely limited, compared with these Tg models, were particularly striking. Using a conventional infection with 10^6 *L. major*, OVA-specific IgG1 Ab responses were detected within 2 wk of infection with PHOC *L. major* and increased thereafter. Less abundant and slightly delayed IgG2a responses also were observed, confirming in normal mice the in vivo immunogenicity of OVA when introduced at a physiologic level of expression by these Tg parasites. Importantly, we observed no response to PHOC/GA *L. major* even late in infection when parasite burden in the tissue exceeded 10^{10} amastigotes. Although we cannot rule out bystander help contributing to the generation of these well-defined T-dependent anti-OVA responses, this appears unlikely given the specificity of the responses to cytosolic and plasma membrane OVA described above. Rather, the generation of IgG1 and IgG2a Abs following infection with PHOC, but not PHOC/GA, *L. major* suggests that Ag localization plays a dominant role in the activation of the low frequency of OVA-specific $CD4^+$ T cells present in the unmanipulated repertoire. Thus, dependent on responder T cell frequency and

Ag abundance (i.e., infective dose), Ag localization at the plasma membrane of *L. major* may be an absolute requirement for recognition or provide a significant advantage for $CD4^+$ T cell recognition. It remains to be determined whether the OVA-expressing *L. major* that we have generated here also are effective at inducing activation of OVA-specific $CD4^+$ or $CD8^+$ T cells in the low-dose infection model (36). However, we have demonstrated recently that mice carrying an established infection with OVA- Tg *Leishmania donovani* (generated as described here for PHOC *L. major*), but not with WT *L. donovani* infection, activate adoptively transferred OVA-specific OT-I $CD8^+$ effector and memory T cells, with therapeutic benefit (44).

In conclusion, despite the complexity of Ag processing and presentation in vivo, our data provide, for the first time, a striking demonstration that the subcellular distribution of OVA to the plasma membrane of *L. major*, in the absence of other specific targeting mechanisms, plays a major role in dictating immunogenicity in vivo. This would support suggestions that the lack of proteins on the surface of metacyclic promastigotes or amastigotes has been the result of selective pressures imposed by immune exposure, leaving only those molecules essential for invasion or evasion of the mammalian host (45, 46). Indirectly, therefore, these data support the notion that HASPB plays an important, although as yet undefined, role in host-parasite interactions.

Acknowledgments

We thank Fiona Powrie, Chris Hunter, and Ed Pearce for Tg mice, some obtained through the National Institute of Allergy and Infectious Disease exchange program; the staff of the Biological Services Facility, London School of Hygiene and Tropical Medicine, for animal husbandry; Toni Aebischer and Robert McMaster for gifts of pSS-int and GP63 Ab, respectively; and Paul Denny and other members of the Smith and Kaye groups for providing stimulating discussions.

References

1. Bryant P, Ploegh H. Class II MHC peptide loading by the professionals. Curr. Opin. Immunol. 2004; 16:96–102. [PubMed: 14734116]
2. Ackerman AL, Kyritsis C, Tampe R, Cresswell P. Early phagosomes in dendritic cells form a cellular compartment sufficient for cross presentation of exogenous antigens. Proc. Natl. Acad. Sci. USA. 2003; 100:12889–12894. [PubMed: 14561893]
3. Houde M, Bertholet S, Gagnon E, Brunet S, Goyette G, Laplante A, Princiotta MF, Thibault P, Sacks D, Desjardins M. Phagosomes are competent organelles for antigen cross-presentation. Nature. 2003; 425:402–406. [PubMed: 14508490]
4. Lehner PJ, Cresswell P. Recent developments in MHC-class-I-mediated antigen presentation. Curr. Opin. Immunol. 2004; 16:82–89. [PubMed: 14734114]
5. Dudani R, Chapdelaine Y, Faassen Hv H, Smith DK, Shen H, Krishnan L, Sad S. Multiple mechanisms compensate to enhance tumor-protective $CD8^+$ T cell response in the long-term despite poor $CD8^+$ T cell priming initially: comparison between an acute versus a chronic intracellular bacterium expressing a model antigen. J. Immunol. 2002; 168:5737–5745. [PubMed: 12023374]
6. Garg N, Nunes MP, Tarleton RL. Delivery by *Trypanosoma cruzi* of proteins into the MHC class I antigen processing and presentation pathway. J. Immunol. 1997; 158:3293–3302. [PubMed: 9120286]
7. Kaufmann SH, Hess J. Impact of intracellular location of and antigen display by intracellular bacteria: implications for vaccine development. Immunol. Lett. 1999; 65:81–84. [PubMed: 10065631]
8. Tvinnereim AR, Hamilton SE, Harty JT. Neutrophil involvement in cross-priming $CD8^+$ T cell responses to bacterial antigens. J. Immunol. 2004; 173:1994–2002. [PubMed: 15265934]
9. Kaye PM, Coburn C, McCrossan M, Beverley SM. Antigens targeted to the *Leishmania* phagolysosome are processed for $CD4^+$ T cell recognition. Eur. J. Immunol. 1993; 23:2311–2319. [PubMed: 8103748]

10. Wolfram M, Fuchs M, Wiese M, Stierhof YD, Overath P. Antigen presentation by *Leishmania mexicana*-infected macrophages: activation of helper T cells by a model parasite antigen secreted into the parasitophorous vacuole or expressed on the amastigote surface. Eur. J. Immunol. 1996; 26:3153–3162. [PubMed: 8977317]
11. Wolfram M, Ilg T, Mottram JC, Overath P. Antigen presentation by *Leishmania mexicana*-infected macrophages: activation of helper T cells specific for amastigote cysteine proteinases requires intracellular killing of the parasites. Eur. J. Immunol. 1995; 25:1094–1100. [PubMed: 7737279]
12. McSorley SJ, Asch S, Costalonga M, Reinhardt RL, Jenkins MK. Tracking salmonella-specific CD4 T cells in vivo reveals a local mucosal response to a disseminated infection. Immunity. 2002; 16:365–377. [PubMed: 11911822]
13. Overath P, Aebischer T. Antigen presentation by macrophages harboring intravesicular pathogens. Parasitol. Today. 1999; 15:325–332. [PubMed: 10407380]
14. Lemos MP, Esquivel F, Scott P, Laufer TM. MHC class II expression restricted to CD8α^+ and CD11β^+ dendritic cells is sufficient for control of *Leishmania major*. J. Exp. Med. 2004; 199:725–730. [PubMed: 14993255]
15. Heath WR, Belz GT, Behrens GM, Smith CM, Forehan SP, Parish IA, Davey GM, Wilson NS, Carbone FR, Villadangos JA. Cross-presentation, dendritic cell subsets, and the generation of immunity to cellular antigens. Immunol. Rev. 2004; 199:9–26. [PubMed: 15233723]
16. Henri S, Vremec D, Kamath A, Waithman J, Williams S, Benoist C, Burnham K, Saeland S, Handman E, Shortman K. The dendritic cell populations of mouse lymph nodes. J. Immunol. 2001; 167:741–748. [PubMed: 11441078]
17. Misslitz AC, Bonhagen K, Harbecke D, Lippuner C, Kamradt T, Aebischer T. Two waves of antigen-containing dendritic cells in vivo in experimental *Leishmania major* infection. Eur. J. Immunol. 2004; 34:715–725. [PubMed: 14991601]
18. Henri S, Curtis J, Hochrein H, Vremec D, Shortman K, Handman E. Hierarchy of susceptibility of dendritic cell subsets to infection by *Leishmania major*: inverse relationship to interleukin-12 production. Infect. Immun. 2002; 70:3874–3880. [PubMed: 12065531]
19. Murphy KM, Heimberger AB, Loh DY. Induction by antigen of intrathymic apoptosis of $CD4^+CD8^+TCR^{lo}$ thymocytes in vivo. Science. 1990; 250:1720–1723. [PubMed: 2125367]
20. Da Silva R, Sacks DL. Metacyclogenesis is a major determinant of *Leishmania* promastigote virulence and attenuation. Infect. Immun. 1987; 55:2802–2806. [PubMed: 3666964]
21. Kropf, P.; Brunson, K.; Etges, R.; Muller, I. Immunology of Infection. 1st Ed.. Academic; San Diego, CA: 1998. The *Leishmaniasis* model; p. 419-458.
22. Titus RG, Marchand M, Boon T, Louis JA. A limiting dilution assay for quantifying *Leishmania major* in tissues of infected mice. Parasite Immunol. 1985; 7:545–555. [PubMed: 3877902]
23. Misslitz A, Mottram JC, Overath P, Aebischer T. Targeted integration into a rRNA locus results in uniform and high level expression of transgenes in Leishmania amastigotes. Mol. Biochem. Parasitol. 2000; 107:251–261. [PubMed: 10779601]
24. McKean PG, Denny PW, Knuepfer E, Keen JK, Smith DF. Phenotypic changes associated with deletion and overexpression of a stage-regulated gene family in *Leishmania*. Cell Microbiol. 2001; 3:511–523. [PubMed: 11488813]
25. McKean PG, Delahay R, Pimenta PF, Smith DF. Characterisation of a second protein encoded by the differentially regulated LmcDNA16 gene family of *Leishmania major*. Mol. Biochem. Parasitol. 1997; 85:221–231. [PubMed: 9106195]
26. Nugent PG, Karsani SA, Wait R, Tempero J, Smith DF. Proteomic analysis of *Leishmania mexicana* differentiation. Mol. Biochem. Parasitol. 2004; 136:51. [PubMed: 15138067]
27. Denny PW, Gokool S, Russell DG, Field MC, Smith DF. Acylation-dependent protein export in *Leishmania*. J. Biol. Chem. 2000; 275:11017–11025. [PubMed: 10753904]
28. Price HP, Menon MR, Panethymitaki C, Goulding D, McKean PG, Smith DF. Myristoyl-CoA: protein *N*-myristoyl transferase, an essential enzyme and potential drug target in kinetoplastid parasites. J. Biol. Chem. 2003; 278:7206–7214. [PubMed: 12488459]
29. Stager S, Smith DF, Kaye PM. Immunization with a recombinant stage-regulated surface protein from *Leishmania donovani* induces protection against visceral leishmaniasis. J. Immunol. 2000; 165:7064–7071. [PubMed: 11120835]

30. Lyons AB, Parish CR. Determination of lymphocyte division by flow cytometry. J. Immunol. Methods. 1994; 171:131–137. [PubMed: 8176234]
31. Zaph C, Scott P. Th1 cell-mediated resistance to cutaneous infection with *Leishmania major* is independent of P- and E-selectins. J. Immunol. 2003; 171:4726–4732. [PubMed: 14568948]
32. Kumar S, Tarleton RL. Antigen-specific Th1 but not Th2 cells provide protection from lethal *Trypanosoma cruzi* infection in mice. J. Immunol. 2001; 166:4596–4603. [PubMed: 11254717]
33. Brooks DR, Denise H, Westrop GD, Coombs GH, Mottram JC. The stage-regulated expression of *Leishmania mexicana* CPB cysteine proteases is mediated by an intercistronic sequence element. J. Biol. Chem. 2001; 276:47081–47089.
34. Bird JJ, Brown DR, Mullen AC, Moskowitz NH, Mahowald MA, Sider JR, Gajewski TF, Wang CR, Reiner SL. Helper T cell differentiation is controlled by the cell cycle. Immunity. 1998; 9:229–237. [PubMed: 9729043]
35. Smith KM, Pottage L, Thomas ER, Leishman AJ, Doig TN, Xu D, Liew FY, Garside P. Th1 and Th2 $CD4^+$ T cells provide help for B cell clonal expansion and antibody synthesis in a similar manner in vivo. J. Immunol. 2000; 165:3136–3144. [PubMed: 10975827]
36. Bertholet S, Debrabant A, Afrin F, Caler E, Mendez S, Tabbara KS, Belkaid Y, Sacks DL. Antigen requirements for efficient priming of $CD8^+$ T cells by *Leishmania major*-infected dendritic cells. Infect. Immun. 2005; 73:6620–6628. [PubMed: 16177338]
37. Stegmayer C, Kehlenbach A, Tournaviti S, Wegehingel S, Zehe C, Denny P, Smith DF, Schwappach B, Nickel W. Direct transport across the plasma membrane of mammalian cells of *Leishmania* HASPB as revealed by a CHO export mutant. J. Cell Sci. 2005; 118:517–527. [PubMed: 15657075]
38. Flinn HM, Rangarajan D, Smith DF. Expression of a hydrophilic surface protein in infective stages of *Leishmania major*. Mol. Biochem. Parasitol. 1994; 65:259–270. [PubMed: 7969267]
39. Rangarajan D, Gokool S, McCrossan MV, Smith DF. The gene B protein localizes to the surface of *Leishmania major* parasites in the absence of metacyclic stage lipophosphoglycan. J. Cell Sci. 1995; 108:3359–3366. [PubMed: 8586648]
40. Stager S, Alexander J, Kirby AC, Botto M, Rooijen NV, Smith DF, Brombacher F, Kaye PM. Natural antibodies and complement are endogenous adjuvants for vaccine-induced $CD8^+$ T-cell responses. Nat. Med. 2003; 9:1287–1292. [PubMed: 14502281]
41. Pape KA, Kearney ER, Khoruts A, Mondino A, Merica R, Chen ZM, Ingulli E, White J, Johnson JG, Jenkins MK. Use of adoptive transfer of T-cell-antigen-receptor-transgenic T cell for the study of T-cell activation in vivo. Immunol. Rev. 1997; 156:67–78. [PubMed: 9176700]
42. Filippi C, Hugues S, Cazareth J, Julia V, Glaichenhaus N, Ugolini S. $CD4^+$ T cell polarization in mice is modulated by strain-specific major histocompatibility complex-independent differences within dendritic cells. J. Exp. Med. 2003; 198:201–209. [PubMed: 12860929]
43. Malherbe L, Filippi C, Julia V, Foucras G, Moro M, Appel H, Wucherpfennig K, Guery JC, Glaichenhaus N. Selective activation and expansion of high-affinity $CD4^+$ T cells in resistant mice upon infection with *Leishmania major*. Immunity. 2000; 13:771–782. [PubMed: 11163193]
44. Polley R, Stager S, Prickett S, Maroof A, Zubairi S, Smith DF, Kaye PM. Adoptive immunotherapy against experimental visceral leishmaniasis with $CD8^+$ T cells requires the presence of cognate antigen. Infect. Immun. 2005; 74:773–776. [PubMed: 16369038]
45. Requena JM, Alonso C, Soto M. Evolutionarily conserved proteins as prominent immunogens during *Leishmania* infections. Parasitol. Today. 2000; 16:246–250. [PubMed: 10827430]
46. Chang KP, Reed SG, McGwire BS, Soong L. *Leishmania* model for microbial virulence: the relevance of parasite multiplication and pathoantigenicity. Acta Trop. 2003; 85:375–390. [PubMed: 12659975]

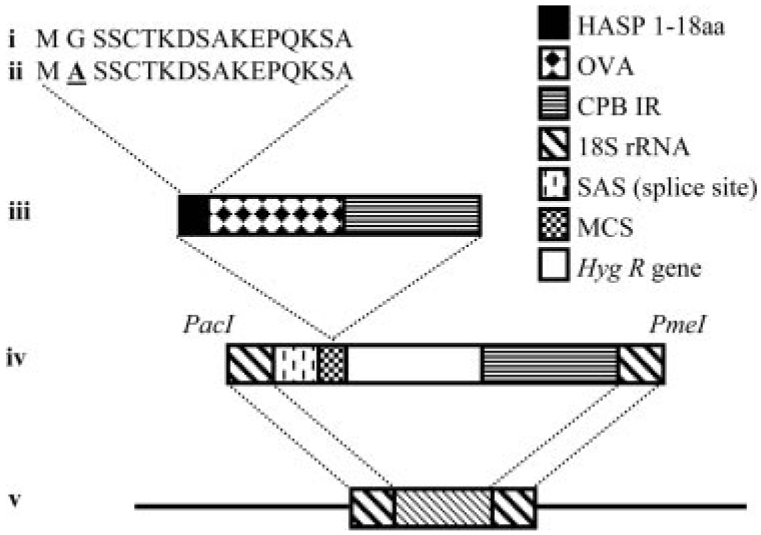

FIGURE 1.

Generation of Tg parasites. PCR was used to amplify the N-terminal 18 codons of *L. major* HASPB (pHOC) (i) or a mutagenized version of the same sequence encoding a Gly-to-Ala switch in the second codon (pHOC/GA) (ii). These HASPB sequences were fused in frame with the OVA ORF immediately upstream of noncoding, regulatory sequences of the *L. mexicana* CPBIR (iii), when cloning into the multiple cloning site of the vector pSSU-int (23) (iv). Vectors were linearized by *Pac*I/*Pme*I digestion (iv) and transfected into *L. major* for targeted integration into a copy of the *18 S rRNA* gene locus (v), generating PHOC and PHOC/GA *L. major*, respectively.

Europe PMC Funders Author Manuscripts

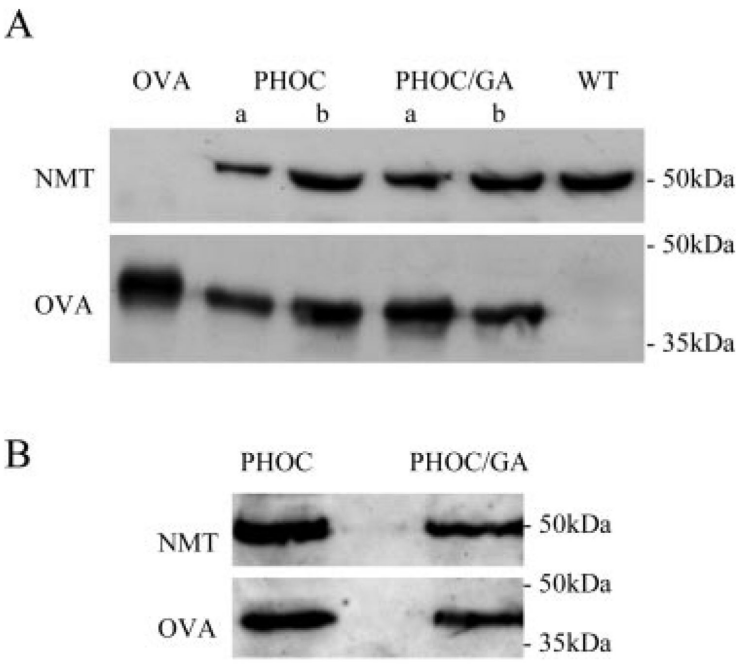

FIGURE 2.

OVA expression in Tg *L. major*. *A*, total cell lysates from ~2 × 10^7 PHOC (two clones, a and b), PHOC/GA (two clones, a and b), or WT (negative control) *L. major* log-stage promastigotes were immunoblotted with goat anti-OVA. A total of 15 ng of OVA was run as a positive control. Rabbit anti-NMT was used as a control for equivalent loading. *B*, Total cell lysates from ~2 ~ 10^7 lesion-derived amastigotes of the PHOC and PHOC/GA a clones were immunoblotted with rabbit anti-OVA. Rabbit anti-NMT was used as a loading control as above.

Europe PMC Funders Author Manuscripts

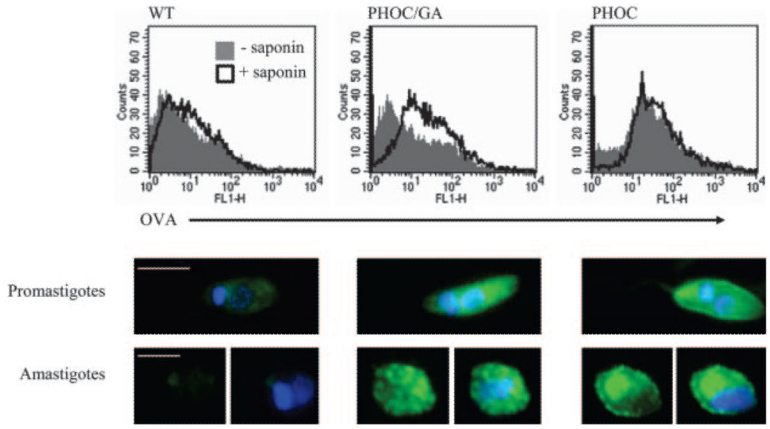

FIGURE 3.

Fluorescent detection of OVA in Tg *L. major*. *Upper panels*, PFA-fixed PHOC, PHOC/GA, or WT *L. major* promastigotes were labeled with goat anti-OVA followed by anti-goat FITC, with or without 0.1% saponin, and analyzed by flow cytometry. Plots show data representative of at least four independent experiments. Log-stage promastigotes and purified metacyclics gave equivalent results. *Lower panels*, PFA-fixed log-stage promastigotes or lesion-derived amastigotes of PHOC, PHOC/GA, or WT *L. major* were labeled with goat anti-OVA followed by biotinylated rabbit anti-goat F(ab′), then Alexa-488-conjugated streptavidin (green). The nuclei and kinetoplasts (blue) were stained with 4′,6′-diamidino-2-phenylindole. Images are representative of multiple parasites from at least two independent experiments; size bars represent 5 and 2.5 μm in promastigotes and amastigotes, respectively.

Europe PMC Funders Author Manuscripts

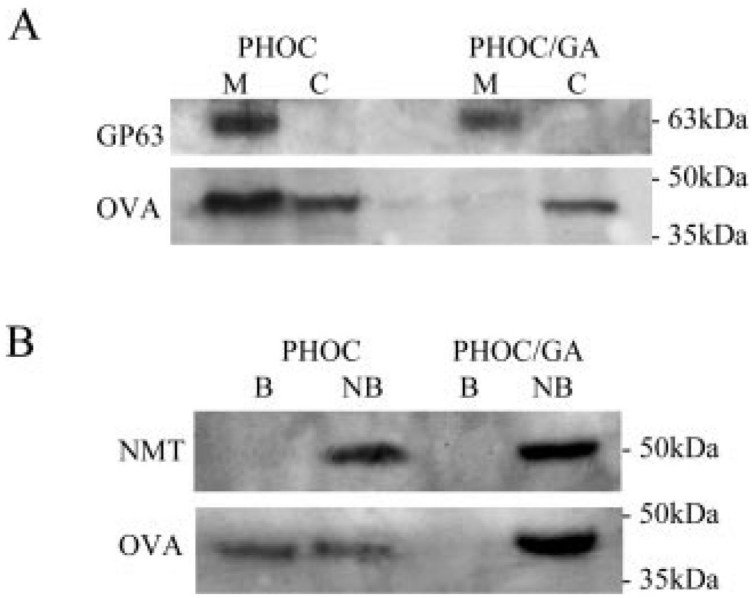

FIGURE 4.

Biochemical analysis of OVA localization. *A*, Membrane fractionation of Tg *L. major.* Total cell lysates of PHOC or PHOC/GA *L. major* were separated into membrane (M) and cytosolic (C) fractions by high-speed ultracentrifugation. Equal amounts of each fraction were used for immunoblotting with goat anti-OVA. Detection of GP63 was used as a loading control and marker for membrane proteins. *B*, Biotinylation of surface-exposed proteins in Tg *L. major.* Surface-exposed proteins of *L. major* log-stage promastigotes were labeled with EZ-link NHS-SS-biotin. Following cell lysis, biotinylated proteins (B) were separated from nonbiotinylated proteins (NB) using streptavidin-agarose beads. Equal amounts of each fraction were used for immunoblotting with goat anti-OVA. Detection of NMT was used as a loading control and marker for internal proteins.

Europe PMC Funders Author Manuscripts

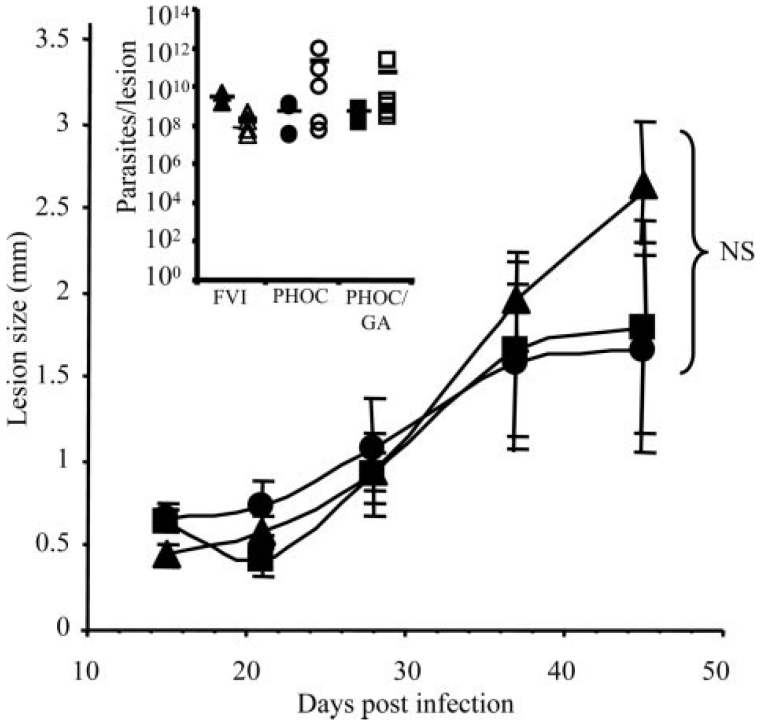

FIGURE 5.

Lesion development in BALB/c mice following infection with Tg *L. major.* Groups of BALB/c mice were infected in one hind footpad with 1×10^6 WT (▲), PHOC (●), or PHOC/GA (■) *L. major* metacyclics. Lesion size was measured by subtracting the thickness of the uninfected footpad from that of the infected footpad. Data show the mean of three to eight mice per group ± SEM and are representative of at least five independent experiments. The insert shows parasite loads in the lesions, as determined by limiting dilution assays at 28 days (closed symbols) and 45 days (open symbols) postinfection. No significant differences in lesion size or parasite load between Tg lines were detected at any time point tested (as measured by Student's *t* test analysis).

Europe PMC Funders Author Manuscripts

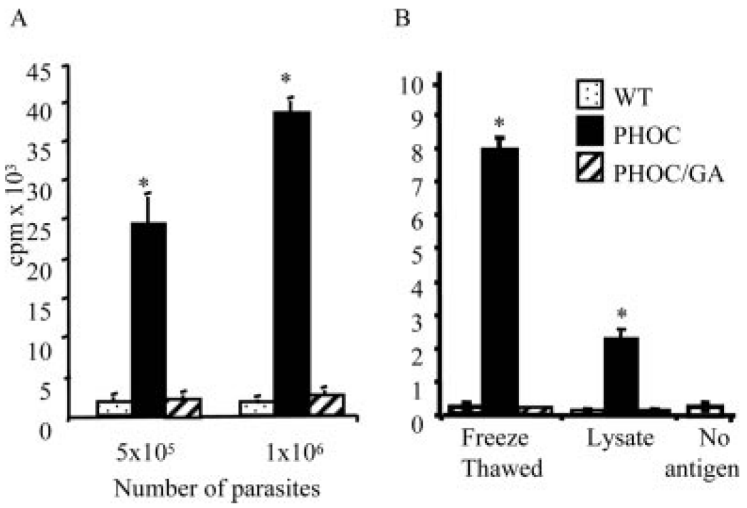

FIGURE 6.

Proliferative responses of DO11.10 T cells generated against Tg *L. major*. A total of 1×10^5 DO11.10 $CD4^+$ T cells were cultured for 96 h with syngeneic splenic DCs pulsed with fixed (*A*) or freeze-thawed (*B*) or soluble lysates of WT FV1, PHOC, or PHOC/GA *L. major* metacyclics. Cells were pulsed with [^{3}H]thymidine for the last 20 h. Data represent the mean of triplicate cultures (±SD) and are representative of at least six independent experiments. Significant differences ($p < 0.005$) are indicated by asterisks. Proliferation in control cultures pulsed with 100 μg/ml soluble OVA or left without Ag were $31.2 \pm 4.4 \times 10^4$ and $2.5 \pm 1.5 \times 10^3$ cpm, respectively.

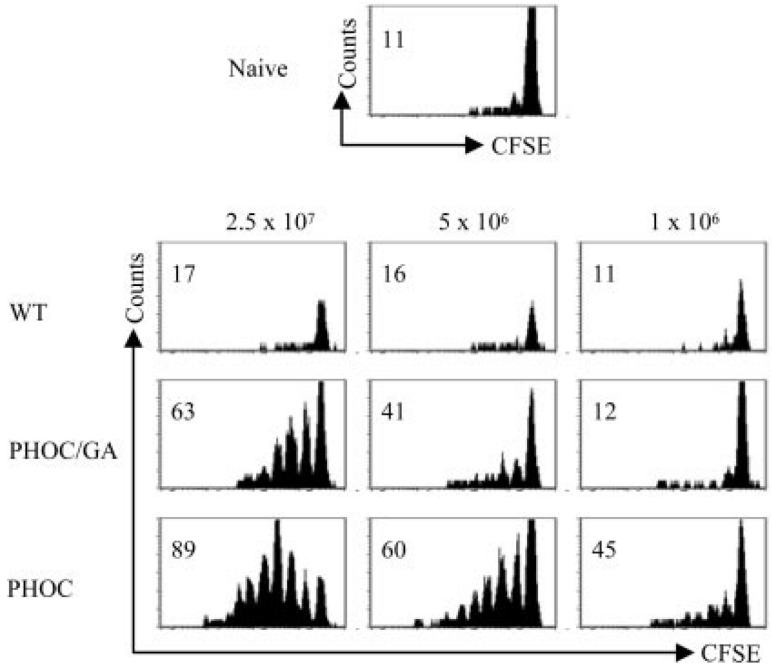

FIGURE 7.

In vivo response of DO.11 T cells to infection with Tg *L. major*. Thy1.1 congenic BALB/c mice received 5×10^6 CFSE-labeled whole splenocytes from DO11.10 (Thy1.2) mice. Recipient mice were infected s.c. in the footpad with 1×10^6–2.5×10^7 WT, PHOC, or PHOC/GA *L. major* metacyclic parasites on the following day. After 4 days, cells were isolated from the draining popliteal lymph node and analyzed by flow cytometry. FACS plots are gated on $KJ126^+CD4^+$ cells. Data are representative of responses observed in at least two mice per group and two independent experiments. Numbers represent the percentage of cells that have diluted CFSE.

Europe PMC Funders Author Manuscripts

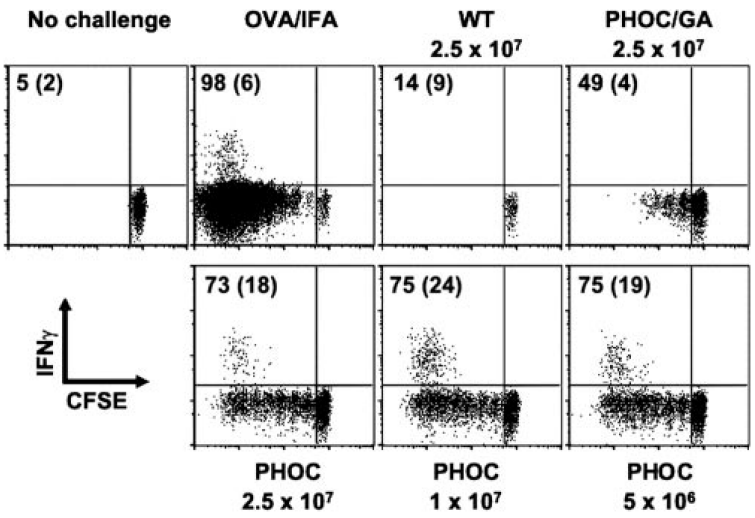

FIGURE 8.

In vivo response of OT-II T cells to infection with Tg *L. major*. Thy1.1 congenic C57BL/6 mice received 5×10^6 CFSE-labeled whole splenocytes from OT-II (Thy1.2) mice. Recipient mice were infected s.c. in the footpad with 5×10^6–2.5×10^7 WT, PHOC, or PHOC/GA *L. major* metacyclic parasites on the following day. Mice were left uninfected or immunized with 50 μg of OVA emulsified in IFA in the footpad as controls. After 4 days, cells were isolated from the draining popliteal lymph node and analyzed by flow cytometry. FACS plots are gated on $CD4^+$ $Thy1.2^+$ cells. Data are representative of responses observed in at least two mice per group and two independent experiments. Numbers represent the percentage of cells that have diluted CFSE (CFSEdim) and the percentage of CFSEdim cells producing IFN-γ (in parentheses).

Europe PMC Funders Author Manuscripts

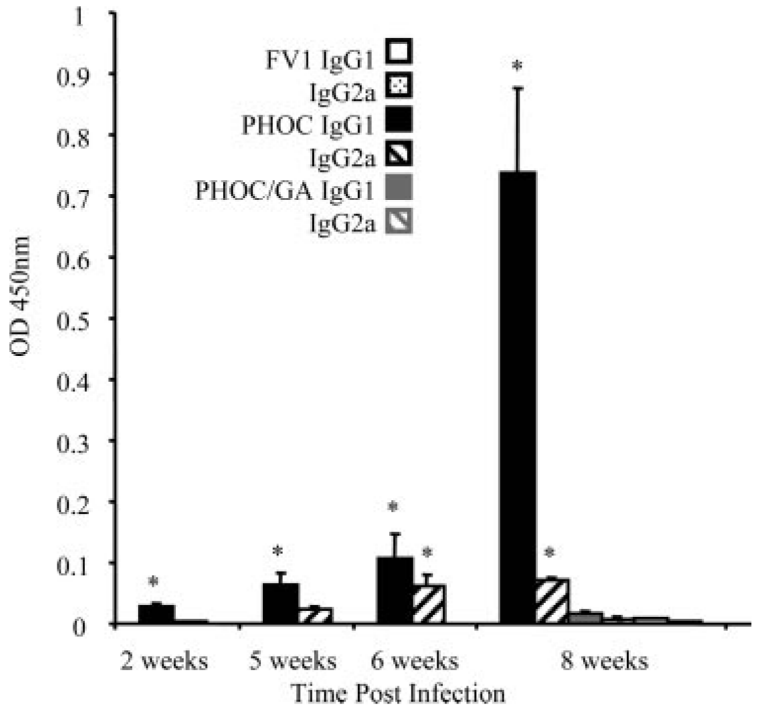

FIGURE 9.

OVA-specific IgG1 and IgG2a responses in infected BALB/c mice. BALB/c mice were infected in one hind footpad with 10^6 PHOC, PHOC/GA, or WT (FV1) *L. major* metacyclics. Relative levels of anti-OVA IgG1 and IgG2a in serum samples from individual mice were determined by ELISA at different times postinfection as indicated. Data show the mean OD ± SD from a 1/160 dilution of serum of groups of three to six mice per time point (taken from the linear range of titrations). Results are representative of three independent experiments. Significant differences ($p < 0.05$) are indicated by asterisks. Maximal responses to infection with WT and PHOC/GA *L. major* are shown at 8 wk only for clarity.

Europe PMC Funders Author Manuscripts